



In situ observation of the reaction of scandium and carbon by neutron diffraction

Erick A. Juarez-Arellano^{a,b,*}, Bjorn Winkler^a, Sven C. Vogel^c, Anatolii Senyshyn^{d,e}, Daniel R. Kammler^f, Miguel Avalos-Borja^{g,1}

^a Institut für Geowissenschaften, Universität Frankfurt, Altenhöferallee 1, 60438 Frankfurt a.M., Germany

^b Universidad del Papaloapan, Circuito Central 200, Parque Industrial, Tuxtpec 68301, Mexico

^c Los Alamos National Laboratory, Lujan Center. Mail Stop H805, Los Alamos, NM 87545, USA

^d Forschungsneutronenquelle Heinz Maier-Leibnitz (FRM II), Technische Universität München, Lichtenbergstr. 1, D-85747 Garching, Germany

^e Materialwissenschaft, TU Darmstadt, Petersenstr. 23, D-64287 Darmstadt, Germany

^f Sandia National Laboratories, Albuquerque, NM 87185, USA

^g CNYN, UNAM, A. Postal 2681, Ensenada, B.C., Mexico

ARTICLE INFO

Article history:

Received 18 April 2010

Received in revised form 11 August 2010

Accepted 24 August 2010

Keywords:

Scandium carbide

Neutron diffraction

ABSTRACT

The formation of scandium carbides by reaction of the elements has been investigated by in situ neutron diffraction up to 1823 K. On heating, the recrystallization of α -Sc occurs between 1000 and 1223 K. The formation of Sc_2C and ScC (NaCl-B1 type structure) phases has been detected at 1323 and 1373 K, respectively. The formation of a new orthorhombic scandium carbide phase was observed at 1473(50) K. Once the scandium carbides are formed they are stable upon heating or cooling. No other phases were detected in the present study, in which the system was always carbon saturated. The thermal expansion coefficients of all phases have been determined, they are constant throughout the temperature interval studied.

© 2010 Elsevier B.V. All rights reserved.

1. Introduction

In comparison to most other transition metal carbides, which are an interesting class of materials with very attractive properties [1], the formation of scandium carbides has not been studied extensively. Phases reported in the Sc–C system include cubic ScC (NaCl-structure type (B1), $a \approx 4.51 \text{ \AA}$ [2,3]), cubic $\text{ScC}_{0.3-0.5}$ (NaCl-structure type (B1), $a \approx 4.7 \text{ \AA}$ [4]), cubic Sc_2C_3 (Pu_2C_3 -type structure, $a = 7.205 \text{ \AA}$ [4]), cubic Sc_4C_3 (Th_3P_4 -structure type, $a = 7.207 \text{ \AA}$ [5]), cubic $\text{Sc}_{13}\text{C}_{10}$ (unknown structure type, $a = 8.53 \text{ \AA}$ [6]) and tetragonal Sc_3C_4 ($P(4/m)nc$, $a = 7.4873 \text{ \AA}$, $c = 15.026 \text{ \AA}$ [7]). In a previous study, we have shown, based on DFT results, that Sc_2C_3 is unlikely to exist and that the sample studied was probably Sc_4C_3 [8].

However, despite the studies mentioned above, it is probably fair to say that the Sc–C system has not been fully explored yet. Specifically, there have been no high temperature in situ investigations at ambient pressure and, hence, the possible formation of intermediate products during the synthesis process has not been investigated. Also, no information related to accurate formation temperatures is available. In this work we followed the reaction

of nominally pure Sc and C from the elements through in situ neutron diffraction measurements, in order to better understand the formation process.

2. Experimental

2.1. Sample

Cryogenic milled scandium metal pieces with a nominal purity of 99.7 wt.% (Alfa Aesar in Ward Hill) and graphite (20 μm grain size) were used in this study. Both materials were previously characterised by Kammler et al. [9] (Sc) and Winkler et al. [10] (graphite). In all the experiments an excess of carbon was used. Additional sample characterisation was performed using electron energy loss spectroscopy (EELS) at the Institute for Scientific and Technological Research of San Luis Potosi (IPICYT) in San Luis Potosi (Mexico) with a Gatan image filter system mounted on a Tecnai G2 F30 operated at 300 kV, with a spherical-aberration coefficient (C_s) of 1.2 mm.

2.2. In situ neutron diffraction

To investigate the reaction of scandium and carbon by neutron diffraction two different synthesis conditions were used. On one hand, the temperature was increased systematically up to temperatures above the scandium melting point (1823 K) in order to get the scandium reacted completely. While on the other hand, once the onset of the reaction of scandium and carbon was detected, the temperature was kept constant in order to see the thermal stability of the first formed phases (HIPPO). Powder neutron diffraction measurements were performed with SPODI [11] diffractometer at the FRM-II reactor (Garching, Germany) and with the HIPPO time-of-flight diffractometer [12] at the Lujan Center at Los Alamos [13]. For the experiments on SPODI, the starting mixture was placed in a corundum crucible which was placed in a niobium holder. In situ powder neutron diffraction measurements were performed using a niobium furnace operated under a vacuum of $<10^{-4}$ Torr and a wavelength of $\lambda = 1.548 \text{ \AA}$. Temperatures were obtained from two

* Corresponding author at: Institut für Geowissenschaften, Universität Frankfurt, Altenhöferallee 1, 60438 Frankfurt a.M., Germany.

E-mail address: eajuarez@unpa.edu.mx (E.A. Juarez-Arellano).

¹ On sabbatical leave at IPICYT, San Luis Potosi, Mexico.

W–Re thermocouples. Counting times varied between 4 and 8 h. The highest temperature at which data was collected was 1823 K. The angular range $2\theta=0\text{--}160^\circ$ was scanned with a step size of 0.05° . The quasi two-dimensional data set was corrected for efficiency and geometrical aberration which are intrinsic for each collimator–detector pair. For the experiments on HIPPO, the starting mixture was placed in a corundum crucible. In situ powder neutron diffraction measurements were performed under a vacuum of $<10^{-5}$ Torr. Temperatures were obtained from two thermocouples in the vicinity of the hot zone and a thermocouple placed in contact with the sample. Data was collected every 20 min. The temperature was increased at 20 K/min up to 1423 K, kept at this temperature for ~ 500 min, and then slowly cooled down. Final powder patterns were obtained by integration along the Debye–Scherrer cones. Data analysis was performed with GSAS [14] and Fullprof [15].

3. Results and discussion

It has been shown that the physical properties of scandium depend on its purity [16]. As scandium is known to have a strong affinity to oxygen, we searched for the most obvious contaminants, i.e., oxygen and nitrogen (from the cryogenic milling process) by EELS. EELS spectra from a piece of scandium in the 300–600 eV energy window shows the scandium L_2L_3 peaks and a small oxygen K-peak (Fig. 1). The nitrogen K-peaks were not observed. Thus, although small amounts of oxygen were observed in the sample, oxygen contamination will not play a role in the reaction of scandium and carbon of this study. The lattice parameters of scandium obtained in this study ($a=3.3072(1)\text{Å}$ and $c=5.2665(4)\text{Å}$) are in agreement both with the data of Kammler et al. [9] and with data published in the literature.

The lattice parameters of the structures discussed here at some selected temperature conditions are shown in Table 1. Some of these values (e.g., for Al_2O_3) have been used as internal standards, from which we have ascertained the accuracy of our results.

At ambient conditions and prior to heating, the diffractograms obtained could be fully indexed by an assignment of peaks to graphite, $\alpha\text{-Sc}$, Al_2O_3 (from the crucible), Nb (from the crucible holder, SPODI) or $\gamma\text{-Fe}$ (from the sample holder, HIPPO). As an example, Fig. 2 shows a fully indexed diffraction pattern obtained at SPODI.

No significant change was observed in the diffraction pattern upon heating up to 1000 K. Between 1000 and 1223 K very

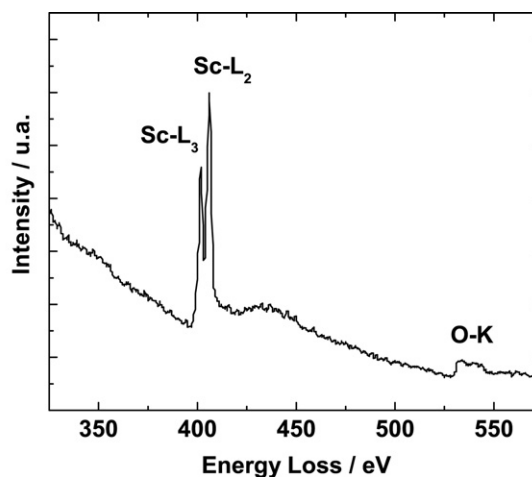


Fig. 1. EELS spectrum from a piece of scandium shows peaks associated with scandium and oxygen in the 300–600 eV window.

well defined and intense spots started to appear in the $\alpha\text{-Sc}$ Debye–Scherrer cones on the SPODI instrument (Fig. 3). We interpret this as the beginning of grain coarsening due to a secondary recrystallization process of $\alpha\text{-Sc}$. The melting point of scandium is 1814 K. Our observation of the grain coarsening at this temperature is therefore consistent with the general tendency of metals to show secondary crystallisation around 0.4–0.5 of their melting temperature.

The onset of the reaction between $\alpha\text{-Sc}$ and graphite was detected at 1323 K (HIPPO) and at 1373 K (SPODI) with the formation of cubic ScC (NaCl-B1 type structure). Neutron diffraction patterns obtained at HIPPO before (1223 K) and after (1423 K) the reaction are shown in Fig. 4. Although the synthesis conditions were rather similar in the two experiments, a Rietveld refinement of the products showed that on HIPPO we have synthesized $\text{ScC}_{0.50}$ (Sc_2C), while the experiment on the SPODI diffractometer resulted in $\text{ScC}_{0.97}$ (ScC). The statistical uncertainty of the carbon site occupancy factor is about 0.02–0.04 in these cases. The

Table 1
Lattice parameters of the structures discussed here at some selected temperature conditions.

Phase ^a	$a/\text{Å}$	$c/\text{Å}$	$V/\text{Å}^3$	Comment
Al_2O_3	4.8061(5)	13.125(2)	262.56(7)	
C	2.4699(6)	6.946(2)	36.70(2)	HIPPO
$\alpha\text{-Sc}$	3.3503(7)	5.388(1)	52.37(2)	1423 K
Sc_2C	4.747(1)	–	106.95(7)	
Al_2O_3	4.8064(1)	13.1357(1)	262.798(2)	
Nb	3.3339(1)	–	37.056(2)	
C	2.459(1)	6.978(2)	36.56(3)	SPODI
$\alpha\text{-Sc}$	3.3482(2)	5.3890(7)	52.267(9)	1523 K
ScC_1	4.5434(4)	–	93.78(3)	
Ortho- ScC_x	15.797(1)	3.9244(3)	592.48(8)	Ortho- ScC_x ; $b=9.5565(7)\text{Å}$
Al_2O_3	4.8198(1)	13.1761(1)	265.078(3)	
Nb	3.3421(1)	–	37.331(2)	SPODI
$\alpha\text{-Sc}$	3.3466(5)	5.3403(5)	51.79(1)	1823 K
ScC_1	4.5615(2)	–	94.914(6)	
Ortho- ScC_x	15.8813(5)	3.9287(2)	596.89(4)	Ortho- ScC_x ; $b=9.5665(4)\text{Å}$
Al_2O_3	4.7578(1)	12.9936(1)	254.723(3)	
Nb	3.3001(1)	–	35.941(2)	SPODI
C	2.4624(7)	6.736(9)	35.374(3)	Ambient temperature
$\alpha\text{-Sc}$	3.2807(3)	5.2484(4)	48.921(8)	After cooling
ScC_1	4.4961(1)	–	90.885(2)	$x \approx 1.0$
Ortho- ScC_x	15.6487(5)	3.8846(1)	569.39(4)	Ortho- ScC_x ; $b=9.3885(1)\text{Å}$
Al_2O_3	4.7672(7)	12.997(3)	255.80(6)	HIPPO
C	2.4932(9)	6.752(3)	36.37(3)	Ambient temperature
$\alpha\text{-Sc}$	3.3202(3)	5.279(4)	50.40(3)	After cooling
Sc_2C	4.7285(4)	–	105.73(3)	$x \approx 0.50$

^a Al_2O_3 ($R\bar{3}c$), C ($P6_3/mc$), $\alpha\text{-Sc}$ ($P6_3/mc$), ScC_x ($Fm\bar{3}m$), Nb ($Im\bar{3}m$) and Ortho- ScC_x ($Pmmm$).

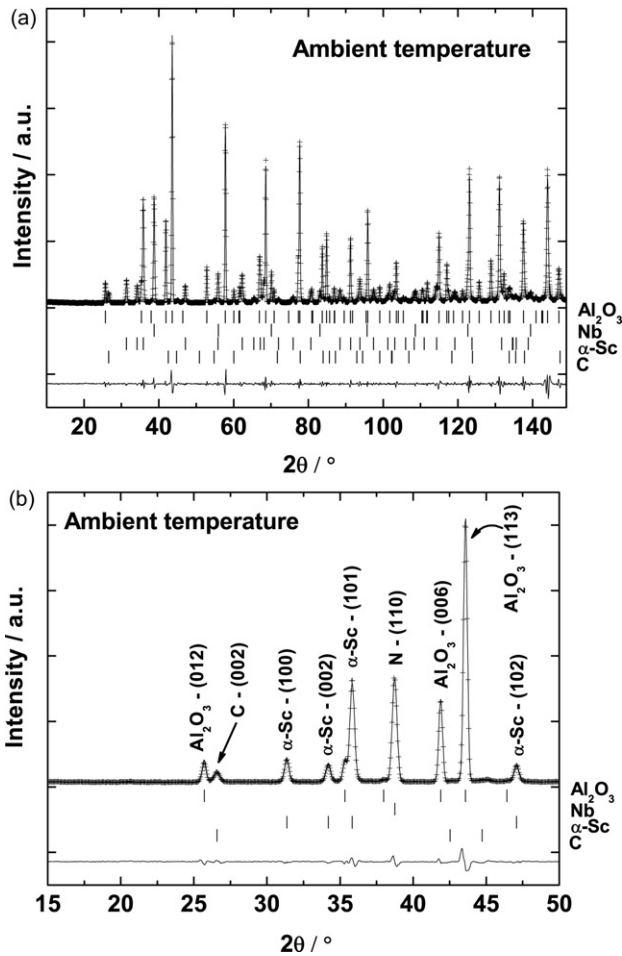


Fig. 2. Rietveld refinement of the neutron diffraction data obtained at SPODI at ambient temperature (left) and an enlargement in the low 2θ region (right).

atomic displacement parameters and the site occupancy factors are, as usual, strongly correlated. At ambient conditions, the atomic displacement parameters can be constrained by comparison to parameters of other structures, but at high temperatures, this cannot be done with confidence. In fact, a variation of the U_{iso} of carbon in scandium carbide in a large range around a realistic value of 0.01 leads to only very small changes in the resultant site occupancy. Hence, while in Rietveld refinements it is generally problematic to extract site occupancies, in the present case we are confident that the two phases indeed have the compositions $ScC_{\approx 1}$ and $ScC_{\approx 0.5}$ (Sc_2C). Both these two phases have been observed before [2–4] and can be clearly distinguished by their lattice parameters. There was a suggestion by Rassaerts et al. [4] that the ScC phase is formed at high temperatures (>2000 K), while the Sc_2C phase is formed around 1473–1773 K and decomposes at higher temperatures. Regrettably, due to time constraints, we could not collect diffraction data in

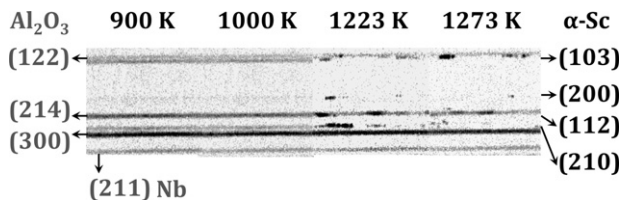


Fig. 3. Selected Debye–Scherrer cones as recorded on the detector (SPODI) before and during the α -Scandium recrystallization. The recrystallization occurred when heating from 1000 to 1223 K.

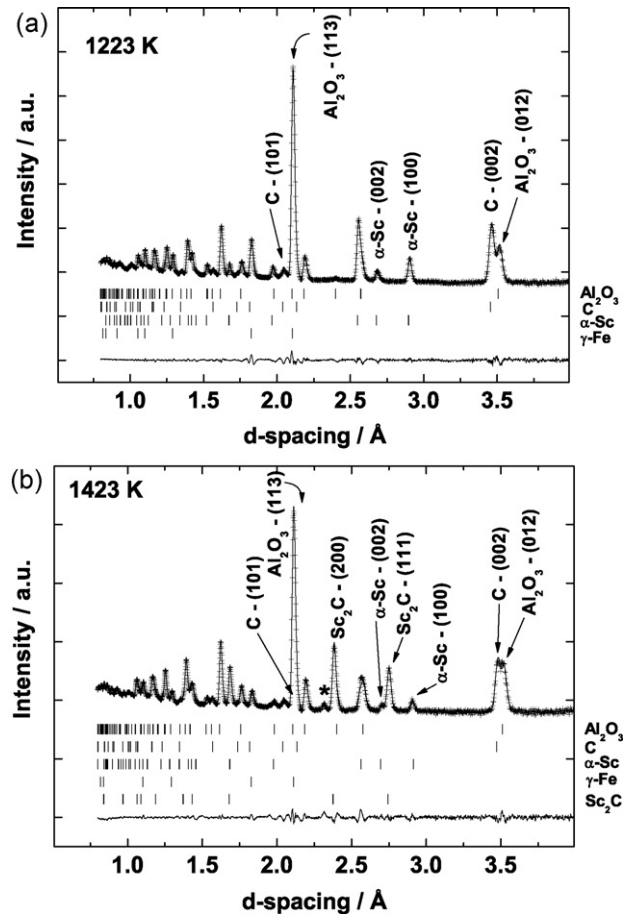


Fig. 4. Neutron diffraction patterns obtained at HIPPO before (1223 K) and after (1423 K) the reaction of α -Sc and graphite. Cubic Sc_2C ($Sc_{0.5}$ (NaCl-B1 type structure) is formed. The star represent an unindexed reflection ($d=2.31$ Å, Ortho- ScC_x -620).

smaller temperature intervals in order to resolve if first Sc_2C is formed which then transforms to ScC. However, the current experiments show that the formation of the B1-structure type cubic scandium carbides from the elements occurs at significantly lower temperatures than was suggested by Rassaerts et al. [4]. Also, once either of the Sc_2C or ScC is formed, it remains stable even during comparatively slow cooling. Although the structures differ only in the site occupancy of the carbon position, the current experiments clearly show that compounds with an intermediate carbon content between $ScC_x \approx 0.5 < x < 1$ are not formed.

At around 1423 K during the experiment at HIPPO and at 1523 K at SPODI several new reflections started to appear. These new reflections cannot be indexed with any of the reported scandium carbide phases (Sc_4C_3 , $Sc_{13}C_{10}$ or Sc_3C_4). A small section of the patterns collected at SPODI shows the formation and evolution of the new reflections as a function of temperature (Fig. 5). Several authors of earlier studies mentioned the existence of reflections that they were unable to index [4–6]. In the current study, it was the superior signal-to-noise ratio of SPODI which allowed a successful indexing. For example, while on HIPPO a single new reflection was observed ($d=2.31$ Å at 1423 K, Fig. 4), several new reflections were observed at SPODI due to its higher signal-to-noise ratio (Fig. 5). Once the new phase is formed, it is stable upon heating (up to 1823 K) and cooling (down to ambient conditions). The new reflections, at ambient conditions, were indexed using the Dicol program [17]. The positions and the relative intensities of these reflections are shown in Table 2. The higher figure-of-merit solution $M_{19}=69.6$ and $F_{19}=34.6$ showed an orthorhombic unit cell with

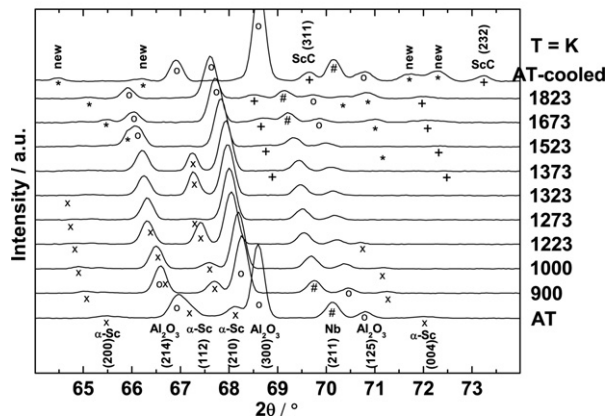


Fig. 5. Section of neutron diffraction patterns as a function of temperature collected at SPODI. At 1373 K started the formation of ScC (ScC_1) (NaCl-B1 type structure) and at 1523 K the formation of a new orthorhombic phase (Ortho- ScC_x).

$a \sim 3.87 \text{ \AA}$, $b \sim 9.36 \text{ \AA}$ and $c \sim 15.65 \text{ \AA}$. The final fitting and the refined unit-cell parameters are shown in Fig. 6 and Table 1, respectively. Le Bail fits were performed in all the neutron diffraction patterns, were the new phase was detected, using this unit-cell (Table 1). Due to the absence of systematic extinctions, the space group $Pmmm$ was chosen. It is worth to mention that the most intense reflection of the new orthorhombic phase (Ortho- ScC_x -(620)) has a d -spacing value similar to the d -value of the single new reflection observed at HIPPO at similar temperatures (Figs. 4 and 7).

The time–temperature diagram of the HIPPO experiment is shown in Fig. 7. From this figure it can be seen that once formed,

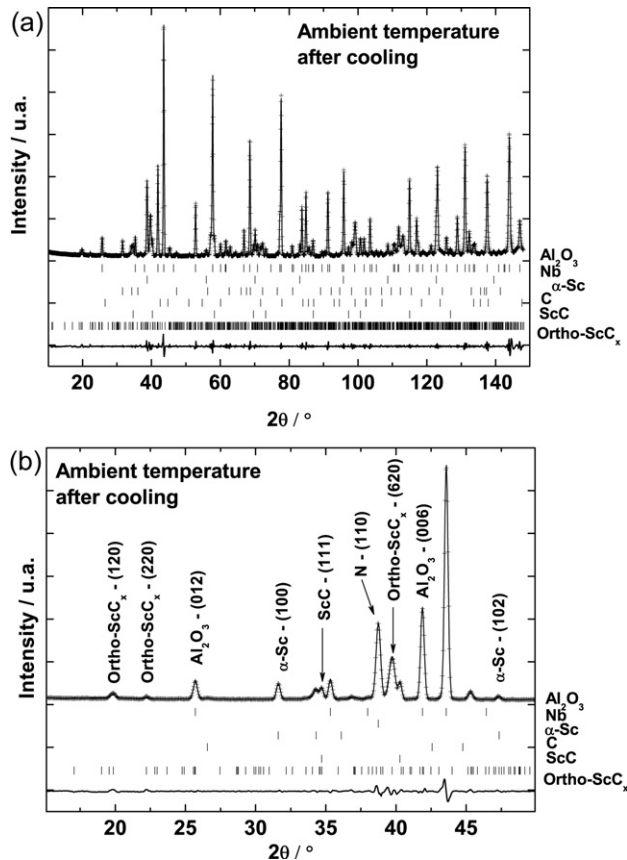


Fig. 6. Full diffractogram obtained at SPODI at ambient temperature after cooling the sample (left) and an enlargement in the low 2θ region (right).

Table 2

Position and relative intensities of the new reflections observed at SPODI (ambient temperature) and the calculated values after indexing them with the unit cell $a = 3.8778(2) \text{ \AA}$, $b = 9.3596(2) \text{ \AA}$ and $c = 15.6559(3) \text{ \AA}$ using Dicvol.

$d_{\text{obs}}/\text{\AA}$	$d_{\text{cal}}/\text{\AA}$	$2\theta_{\text{obs}}$	$2\theta_{\text{cal}}$	Int-f	(hkl)
4.48405	4.48417	19.879	19.879	8.8	(120)
4.01814	4.01705	22.212	22.218	1.6	(220)
2.64275	2.64278	34.061	34.060	7.5	(411)
2.33994	2.34000	38.632	38.631	29.5	(040)
2.27903	2.27910	39.707	39.706	100.0	(620)
2.01808	2.01802	45.105	45.107	1.2	(720)
2.00836	2.00844	45.336	45.334	12.8	(440)
1.62344	1.62351	56.949	56.946	1.1	(512)
1.61681	1.61683	57.204	57.203	38.0	(740)
1.51935	1.51938	61.251	61.250	1.8	(930)
1.48435	1.48437	62.858	62.857	8.7	(551)
1.45181	1.45178	64.434	64.436	5.0	(1001)
1.41604	1.41601	66.267	66.269	3.8	(651)
1.32130	1.32132	71.717	71.716	10.1	(822)
1.31377	1.31373	72.192	72.195	2.6	(561)
1.24793	1.24791	76.665	76.667	2.6	(271)
1.21060	1.21061	79.487	79.486	3.1	(951)
1.13761	1.13762	85.746	85.745	6.1	(671)
1.09005	1.09002	90.479	90.482	9.3	(272)

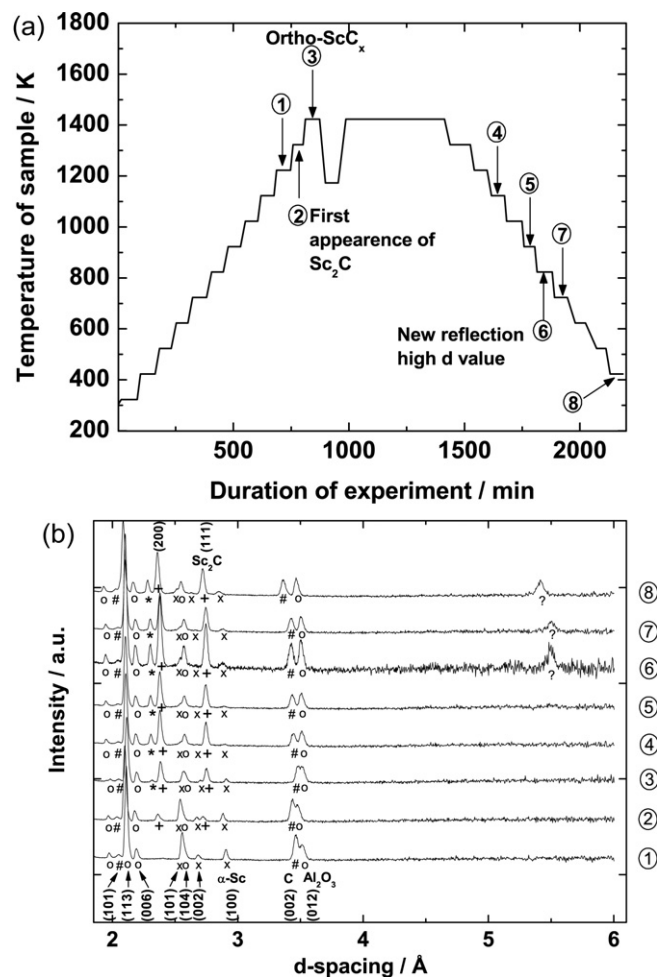


Fig. 7. (Upper panel) time–temperature diagram of the HIPPO experiment. (Lower panel) sections of neutron diffraction patterns according to the time marked in the diagram. The Ortho- ScC_x -(620) reflection appeared at 1423 K ($d = 2.31 \text{ \AA}$). A new unknown reflection appears after keeping the sample at 1423 K for more than 500 min.

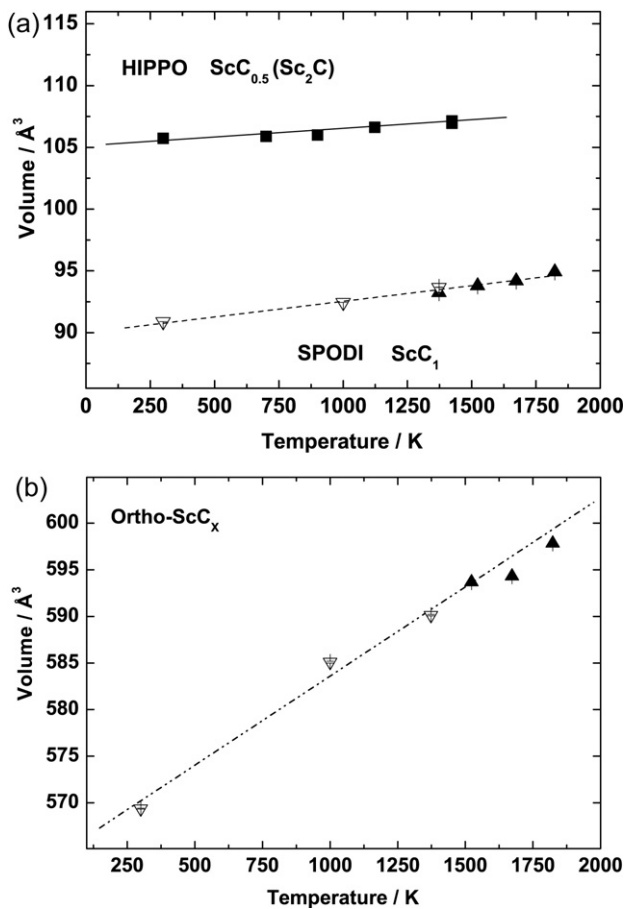


Fig. 8. Temperature dependence of the unit cell volume of ScC , Sc_2C and orthorhombic ScC_x . Open and filled symbols represent data collected during cooling and heating, respectively. Lines are guides to the eye.

all the phases are stable. However, after around 500 min one new unknown reflection appears at $d = 5.51 \text{ \AA}$. This reflection is observed through the rest of the experiment (Fig. 7). Unfortunately, no other reflection was detected, and hence it could not be indexed. However, it is known that defects may order or disorder depending on the composition and thermal treatment the ordering may form new lattices [18]. Krikorian et al. [5,6] observed non-indexed reflections in samples annealed ex situ at 1323 K for 254–280 h and in samples with a minor addition of Ge annealed ex situ at 1273–1923 K for 2–168 h. Therefore, we think that the appearance of new reflections with annealing is related to the ordering of vacancies in the existing phases rather than further reaction of scandium and graphite.

3.1. ScC , Sc_2C and orthorhombic ScC_x thermal expansion

The temperature dependence of the unit cell volume of the two B1-type structure (ScC , Sc_2C) phases and the new orthorhombic ScC_x phase are shown in Fig. 8. The volume thermal expansion of all the phases is constant within the experimental errors throughout the temperature interval studied here. For the ScC and Sc_2C phases we obtained a thermal volumetric expansion coefficient of $\alpha_V = 29.11(7) \times 10^{-6} \text{ K}^{-1}$ (ScC , SPODI) and $\alpha_V = 10.28(4) \times 10^{-6} \text{ K}^{-1}$ (Sc_2C , HIPPO), while for the orthorhombic ScC_x a coefficient of $\alpha_V = 32.78(4) \times 10^{-6} \text{ K}^{-1}$. The thermal linear expansion coefficient of the orthorhombic ScC_x phase are $\alpha_a = 9.76(2) \times 10^{-6} \text{ K}^{-1}$, $\alpha_b = 14.03(1) \times 10^{-6} \text{ K}^{-1}$, $\alpha_c = 7.42(3) \times 10^{-6} \text{ K}^{-1}$. These values are similar to the thermal expansion of TiC , where Winkler et al. [10] obtained $\approx 30 \times 10^{-6} \text{ K}^{-1}$.

4. Conclusions

In the present study, we have determined the temperature at which the reaction of scandium and graphite commences to form scandium carbide. In agreement with earlier studies we found that there are two cubic phases with the B1-structure type, which differ in the site occupancy of the carbon position. Our results show that there is no continuous filling of the carbon site. The temperature resolution of our study was insufficient to unambiguously determine if the partially filled $\text{ScC}_{0.5}$ (Sc_2C) is first formed and then, at only marginally higher temperatures, transforms to ScC_1 . This would require a further in situ study at more closely spaced temperature intervals. Also, currently an understanding on why there is an absence of phases with an “intermediate” carbon content is elusive. Furthermore, our study has shown that there is a new orthorhombic scandium carbide whose structure remains to be determined. Hence, while the present study has answered some questions and provided new data on the formation of scandium carbides, numerous new questions require further studies.

Acknowledgements

This research was supported by Deutsche Forschungsgemeinschaft (Project Wi-1232), in the framework of the DFG-SPP 1236. This research was partially supported by DGAPA-UNAM grant IN-108908 and CONACyT-DAAD PROALMEX grant. LANL is operated by the Los Alamos National Security LLC under the DOE Contract of DE-AC52-06NA25396. The Lujan Neutron Scattering Center at the Los Alamos Neutron Science Center is funded by the Department of Energys Office of Basic-Energy Science. Sandia is a multiprogram laboratory operated by Sandia Corporation, a Lockheed Martin Company, for the United States Department of Energy (DOE) under Contract No. DE-AC04-94AL85000.

Appendix A. Supplementary data

Supplementary data associated with this article can be found, in the online version, at doi:10.1016/j.jallcom.2010.08.081.

References

- [1] H.O. Pierson, Handbook of Refractory Carbides, Noyes Publication, 1996.
- [2] H. Auer-Welsbach, H. Nowotny, Monatshefte für Chemie 92 (1961) 198–201.
- [3] H. Nowotny, H. Auer-Welsbach, Monatshefte für Chemie 92 (1961) 789–793.
- [4] H. Rassaerts, H. Nowotny, G. Vinek, F. Benesovsky, Monatshefte für Chemie 98 (1967) 460–468.
- [5] N.H. Krikorian, A.L. Bowman, M.C. Krupka, G.P. Arnold, High Temperature Science 1 (1969) 360–366.
- [6] N.H. Krikorian, A.L. Giorgi, E.G. Szklarz, M.C. Krupka, Journal of the Less-Common Metals 19 (1969) 253–257.
- [7] R. Pöttgen, W. Jeitschko, Inorganic Chemistry 30 (1991) 427–431.
- [8] E.A. Juarez-Arellano, B. Winkler, L. Bayarjargal, A. Friedrich, V. Milman, D.R. Kammler, S.M. Clark, J. Yan, M. Koch-Müller, F. Schröder, M. Avalos-Borja, Journal of Solid State Chemistry 183 (2010) 975–983.
- [9] D.R. Kammler, M.A. Rodriguez, R.G. Tissot, D.W. Brown, B. Clausen, T.A. Sisneros, Metallurgical and Material Transactions A 39A (2008) 2815–2819.
- [10] B. Winkler, D.J. Wilson, S.C. Vogel, D.W. Brown, T.A. Sisneros, V. Milman, Journal of Alloys and Compounds 441 (2007) 374–380.
- [11] M. Hoelzel, A. Senyshyn, R. Gilles, H. Boysen, H. Fuess, Neutron News 18 (4) (2007) 23–27.
- [12] H.R. Wenk, L. Lutterotti, S.C. Vogel, Nuclear Instruments and Methods in Physics Research A 515 (2003) 575–588.
- [13] P.W. Lisowski, C.D. Bowman, G.J. Russell, S.A. Wender, Nuclear Science and Engineering 106 (1990) 208–218.
- [14] A. Larson, R. Von Dreele, Los Alamos National Laboratory Report LAUR 86-748 (2004).
- [15] J. Rodriguez-Carvajal, Physica B 192 (1993) 55–69.
- [16] E.V. Galoshina, V.P. Dyakina, V.E. Startsev, The Physics of Metals and Metallography 83 (1996) 248–263.
- [17] A. Boulif, D. Louer, Journal of Applied Crystallography 37 (2004) 724–731.
- [18] C.H. Novion, J.P. Landesman, Pure and Applied Chemistry 57 (1985) 1391–1402.